Aging near rough and smooth boundaries in colloidal glasses

Cong Cao, Xinru Huang, Connie B. Roth, and Eric R. Weeks
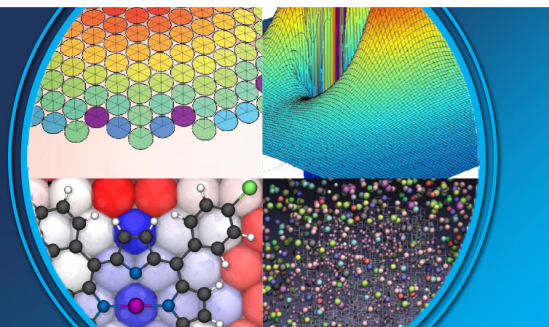
Aging near rough and smooth boundaries in colloidal glasses

Cong Cao,[a)] Xinru Huang, Connie B. Roth, and Eric R. Weeks[b)]

Department of Physics, Emory University, Atlanta, Georgia 30322, USA

We use a confocal microscope to study the aging of a bidisperse colloidal glass near rough and smooth boundaries. Near smooth boundaries, the particles form layers, and particle motion is dramatically slower near the boundary as compared to the bulk. Near rough boundaries, the layers nearly vanish, and particle motion is nearly identical to that of the bulk. The gradient in dynamics near the boundaries is demonstrated to be a function of the gradient in structure for both types of boundaries. Our observations show that wall-induced layer structures strongly influence aging. *Published by AIP Publishing.* https://doi.org/10.1063/1.5000445

I. INTRODUCTION

Glasses are solids with disordered structures and slow internal dynamics. Efforts to understand the influence of boundaries on glassy dynamics has been an active area of research for more than two decades.[1–8] Initial efforts on confined systems were thought to provide a route to accessing postulated growing length scales associated with cooperative motion.[5,9–16] However, the study of such small system sizes necessitates the presence of boundaries and it has turned out that the specific details of such interfaces have a great deal of influence on the local dynamics near the boundary.[17] In experimental material systems, the type of interface often plays a dominant role over finite size effects where interfacial energy, specific chemical interactions, and substrate compliance are all factors that have been shown to have some influence on the dynamics.[18–29] In computer molecular dynamics (MD) simulations where the specific details of the boundary need to be constructed at its most basic level, it is unclear *a priori* how best to accomplish this.

Early MD efforts started with smooth, structureless walls where the boundary was treated as a continuum and details of the wall potential were integrated over in the lateral (x,y) direction leaving only a z-dependence perpendicular to the boundary.[5] Alternatively, molecularly structured walls assembled from Lennard-Jones (LJ) particles into either crystalline arrays or frozen amorphous structures were also investigated.[10,11,30–33] In these simulations, local dynamics near the boundary were usually different than bulk, but the underlying cause was frequently unclear. Smooth walls typically exhibit faster dynamics than bulk in part because there is no penalty for the particles to slide laterally along the wall,[9,34–37] a type of motion only considered to be experimentally relevant for a free surface.[36] Systems with molecularly structured walls, where lateral sliding is inhibited, typically exhibited slower dynamics in comparison.[10,11,13,30,31,38]

One of the major challenges with such boundaries is that for mixtures of LJ particles or polymeric bead-spring models (the most commonly modeled systems), the presence of the wall creates layering of the particle density $\rho(z)$ as a function of distance from the wall.[5] Intuitively, the particles pack easily in a layer against the wall, and then the particles in the second layer pack against that first layer, etc., with the influence of the wall diminishing farther away. Thus, a major effort in these studies is the need to determine the extent to which the observed differences in local dynamics a distance z to the boundary are influenced by the local $\rho(z)$ structure in density. In some cases, slower dynamics near the boundary has been associated with a significantly increased local density,[5,39] while other studies have demonstrated that the change in dynamics near the boundary is unrelated to the $\rho(z)$ density profile.[10,11,31,37] For example, even efforts to construct a "neutral" boundary that avoids local perturbations to the particle density by freezing in an amorphous, liquid-like structure still leads to perturbations in the local dynamics.[10,11,30,40–43] It is important to note that local perturbations to the $\rho(z)$ structure are not only limited to coarse-grained simulations but are also observed in nearly atomistic, united-atom models.[44] In addition, experimental studies on glassy thin film systems are also trying to uncover the extent to which molecular ordering occurs near a boundary and its possible influence on the local density and dynamics.[45–49]

Here we present a direct experimental comparison of local glassy dynamics next to rough and smooth boundaries using colloidal glasses, which have been previously suggested as a means for experimentally verifying these observations from coarse-grained MD simulations of boundaries.[8,39,50] Colloids are small solid particles in a liquid, where Brownian motion allows particles to diffuse and rearrange.[8] We use a confocal microscope to study the aging of a bidisperse colloidal glass where layer-resolved dynamics as a function of distance from a rough or smooth wall are compared with the measured $\rho(z)$ density profile. Smooth boundaries are simply a normal untreated glass coverslip, while rough boundaries are constructed by melting a small amount of the colloidal sample to the coverslip. These stuck particles cover

a)Electronic mail: ccao8@emory.edu
b)Electronic mail: erweeks@emory.edu

approximately 30%-50% of the surface and provide a roughness scale comparable to the particle size. The particle-glass and particle-particle interactions are purely repulsive and so the main difference in the boundary conditions is the topography. We observe distinctly different results between smooth and rough boundary conditions: near smooth boundaries, motion is dramatically slower, whereas near rough boundaries, the aging process is nearly independent of the distance from the boundary. We ascribe this to the strong influence of layer-like structures formed near the smooth boundary.

Our samples are aging: unlike many phases of matter, glasses are out of equilibrium, and so their properties slowly evolve, perhaps toward a steady state.[51–54] These properties can include the density, enthalpy, and diffusive motion of the molecules comprising the glass. This has implications for the usage of glassy materials which have properties that depend on age perhaps in an undesirable way.[53,55,56] Aging has been observed in polymer glasses,[53,55] granular systems,[57,58] and soft materials such as colloids and foams.[52,59–66] While for polymer glasses and granular materials, aging is often measured as a slight decreases in volume, colloidal glasses are typically studied at constant volume. The main signature of aging of colloidal glasses is the dramatic slowing of particle motion as the sample ages,[52,59,60] often characterized by the slowing down of the mean square particle displacement for time windows at increasing aging times.[62] Previous work suggests that aging in colloidal systems may relate to the local structure around rearranging particles[63] or domains of more mobile particles.[62,67] In general, it is not surprising that confined glasses age in different ways from their bulk counterparts.[53] In this manuscript, we show that the aging of colloidal particles is tied to the layering structure imposed by the nearby sample boundaries.

II. EXPERIMENTAL DETAILS

In our experiment, we use sterically stabilized poly(methyl methacrylate) (PMMA) particles[68,69] to prevent aggregation. Two different sizes of particles are mixed in order to prevent crystallization, with $d_L = 2.52$ μm and $d_S = 1.60$ μm. The particles have a polydispersity of 7%. The number ratio is approximately 1:1. To match the particles' density and refraction, we use a mixture of decalin and cyclohexylbromide as the solvent.[70] We view our samples with a fast confocal microscope (VT-Eye from Visitech, International). The large particles are dyed with rhodamine dye and thus are visible, while the small particles are undyed and thus unseen. Based on prior work, we expect that both small and large particles have similar behavior.[63,71] Visual inspection using a differential interference contrast microscopy, where we can see both particle types, confirms that the particles are well-mixed even at the boundary. The imaged volume is $50 \times 50 \times 20$ μm^3. These images are taken once per minute for 2 h. Our scanning volume starts about 5 μm outside the boundary to ensure that we have clear images of the particles at the boundary. The microscope pixel size is 0.11 μm in x and y (parallel to the boundary) and 0.2 μm in z (perpendicular to the boundary). We use standard software to track the motion of the particles in 3D.[70,72] Our particle locations are accurate to 0.10 μm

initially and to 0.15 μm by the end of the experiment after some photobleaching occurs.

We construct two types of sample chambers. The first uses a normal untreated coverslip as a smooth boundary. The second is prepared by taking a small amount of colloidal sample and melting it onto the coverslip, using an oven at 180 °C for 20 min. After this process, the PMMA particles are irreversibly attached to the coverslip. This sample is the same bidisperse mixture of PMMA particles as the main sample with the exception that both particle sizes are undyed. By image analysis, we determine that the stuck particles cover approximately 30%-50% of the surface. The specific fraction is difficult to measure as we only image the large fluorescently dyed particles, so we cannot see either the smaller mobile particles of our bidisperse sample or the stuck particles of either size. After adding the samples, we never observe any of our sample particles stuck to the boundaries for either smooth or rough boundary conditions.

We add a stir bar inside each sample chamber so that we can shear rejuvenate the samples[62] and thus initiate the aging process and set $t_{age} = 0$ (when we stop stirring). Note that t_{age} is set by the laboratory clock and thus is identical throughout our sample; we are not considering the idea of a spatially varying time scale. We find that the stirring method gives reproducible results similar to prior work,[62,63] although this is probably different from a temperature or density quench as is usually done for polymer and small molecule glasses.[73] Given the flows caused by the stirring take 20-30 s to appreciably decay after stirring is stopped, there is some uncertainty in our $t_{age} = 0$, but we examine the data on time scales at least ten times larger than any uncertainty of this initial time.

The confocal microscope allows us to measure the bulk number density for large particles, which we find to be 0.32 ± 0.03 μm. The uncertainty represents the variability that we see from location to location. Given that we cannot directly observe the small particles, the observed number density in any given location is not a useful measure of the local volume fraction. Thus, we do not have a direct measure of the volume fraction. Given that the samples behave as glasses (to be shown below) and particles are still able to move, we conclude $\phi_{glass} < \phi < \phi_{rcp}$, with $\phi_{glass} \approx 0.58$ (for bidisperse colloidal glasses[71]) and $\phi_{rcp} \approx 0.65$ (the value for random close packing for our bidisperse sample[74]). Prior studies of aging colloidal glasses found little[75] or no[62] dependence of the behavior on ϕ. It is important to note that we cannot definitely establish if our two samples are at the same ϕ or, if not, which one would be higher.

III. RESULTS

Figure 1 shows reconstructed 3D images for smooth (a) and rough (b) boundaries. To show the influence of the boundaries, the particles closest to the boundary are on the top of these pictures (colored dark purple). The color changes continuously as a function of the distance z away from the boundary. However, the particles shown in Fig. 1(a) appear to have discrete colors as they form layers with distinct z values. This phenomenon is induced by the flat wall and is well known.[27,76]
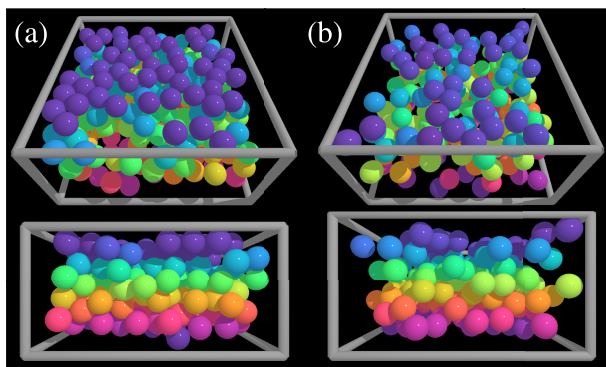
FIG. 1. Top view and side view for reconstructed 3D images for colloidal samples near (a) a smooth boundary and (b) a rough boundary. Color is a continuous parameter representing particles' distances away from the boundary (from 0 to 10 μm). The particles closest to the boundary are on the top and colored dark purple. The grey boxes have dimensions $20 \times 20 \times 15$ μm^3, which is a subset of the full image volume. While the sample has particles of two sizes, only the large particles are visible in the experiment. The data are pictured at $t_{age} = 10$ min.

To quantify the layered structure, we measure the time-averaged number density for the large particles $n(z)$. This is shown in Fig. 2 for smooth (a) and rough (b) boundaries. We set $z = 0$ at the center of the particle whose center is closest to the boundary. The vertical dotted lines indicate the separate layers. As the sample is composed of two sizes of particles, the layer structure decreases rapidly away from the wall, consistent with simulations[77,78] and experiments.[27] The first peak in Fig. 2(a) has the maximum value and minimum width, indicating particles are in a well-defined layer, consistent with Fig. 1(a). By the sixth layer, it is unclear if there is still a layer or if we are seeing random number density fluctuations. For the rough wall in panel (b), the layers become poorly defined by the fourth layer. We extend the definition of layers in the bulk by using a fixed spacing of 1.8 μm; this will facilitate later analysis. Note that for the rough boundary condition, the wall texture occupies some of the space of the first layer, thus decreasing the number of dark purple particles in Fig. 1(b) and reducing the area under the first peak in Fig. 2(b).

Aging manifests as a slow change of sample behavior with increasing t_{age}, where the rate of change slows at longer
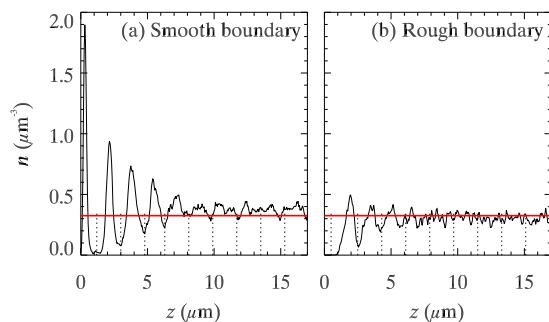

FIG. 2. The local number density $n(z)$ as a function of the distance from the boundary at $z = 0$ μm for samples near (a) a smooth boundary and (b) a rough boundary. Layer-like structures are observed in both samples in the first few layers, although they are sharper for the smooth boundary and persist to larger z. The vertical dotted lines indicate separate layers, with a fixed spacing once the layers become ill-defined. The red horizontal lines show the average number density in the region $z > 10$ μm.

times.[51] The easiest quantity to see this with our data is the mean square displacement (MSD) of particle motion.[63,67] Figure 3 shows the motion parallel to the boundaries for (a,b) rough and (c,d) smooth boundaries, with panels (b) and (d) corresponding to the bulk MSD curves. The different colors indicate different ages. The mean square displacement is computed as $\frac{1}{2}\langle \Delta x^2 + \Delta y^2 \rangle$ where the angle brackets indicate an average over all large particles and over all starting times within the window of t_{age}. For our shortest time scale ($\Delta t = 1$ min), the MSD curves have a shallow slope indicating that the particles are trapped by the local configuration, with the exception of the black curves ($t_{age} \le 8$ min) when the aging has just started. At long time scales, the MSDs show an upturn, which is related to the samples' age.[62,63,67] For larger t_{age}, there is an increase in the time scale Δt needed to reach a given value of the MSD, indicating the slowing particle motion. Note that as we take data, the fluorescent dye in the particles begins to photobleach and our particle tracking resolution worsens, slightly increasing the measured MSD values at small Δt.[79] Slight differences in the image quality may also be affecting the overall height of the MSD curves between the smooth and rough boundary conditions for the data at $\Delta t \le 10$ min.[79] Accordingly, for subsequent analysis below, we will focus on large Δt values for which the signal is greater than the photobleaching noise. The main points to learn from Fig. 3 are that the overall behavior of the curves shows the expected aging trend with larger t_{age}, and panels (b) and (d) show that the aging curves are similar for both boundary conditions far from the boundary.

Figure 3(a) shows the MSD curves for xy motion for the first layer with rough boundary conditions. Surprisingly, there barely exist any differences compared to Fig. 3(b), which depicts the MSDs of the fourth layer. The particles overall show the aging behavior with slower dynamics for larger t_{age}. In contrast to the rough boundary, the MSD curves for the
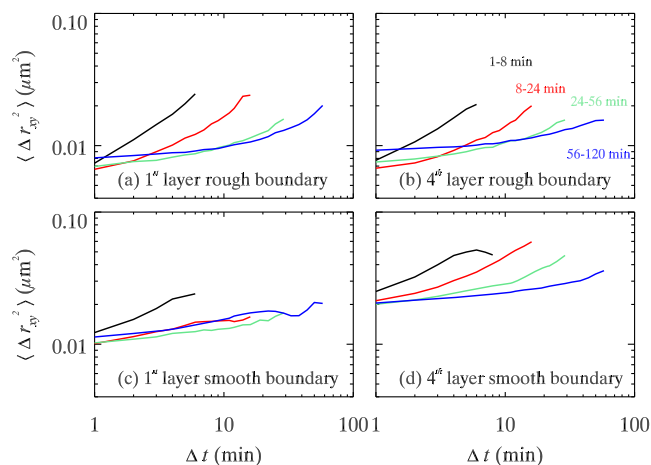

FIG. 3. The mean square displacement for motion parallel to the boundaries calculated as $\langle \Delta r_{xy}^2 \rangle = \frac{1}{2}\langle \Delta x^2 + \Delta y^2 \rangle$. The data are averaged over four different t_{age} regimes as indicated. Data are for (a) 1st layer with a rough boundary, (b) 4th layer with a rough boundary, (c) 1st layer with a smooth boundary, (d) 4th layer with a smooth boundary. The data for the 4th layers match the bulk behavior, and their progression to larger time scales with increasing t_{age} demonstrates that the sample is aging. The data for the 1st layers show that aging is fairly unchanged for the rough boundary (a) but markedly different for the smooth boundary (c).

first layer next to the smooth boundary look strikingly different from the bulk case, as seen by comparing Figs. 3(c) and 3(d). In all four time groups, the MSD curves in the first layer are slightly smaller than those in the fourth layer. The smooth wall greatly restricts particle mobility, similar to what has been seen for dense colloidal liquids near smooth walls.[27] Moreover, unlike the fourth layer, where the MSD curves strictly follow the aging order, the aging process seems to reach a t_{age}-independent state by $t_{age} = 8$ min. This is likely because the dynamics in this layer are extremely slow, including the aging dynamics. This explanation is also consistent with the pronounced first layer density peak seen in Fig. 2(a).

Figure 4 shows the MSD data for the z component of motion, perpendicular to the boundary. The results are similar to the MSD data of Fig. 3, with the exception that the layers closest to the boundaries show less motion [panels (a) and (c)] for both rough and smooth boundary conditions. The increase in the height of the MSD curves with age in Figs. 4(a) and 4(c) is due to photobleaching, but otherwise those MSD curves are fairly flat. Here the first layer for the rough boundary shows some differences with the bulk behavior [compare panels (a) and (b)]. The contrast between the first layer and bulk is stronger for the smooth boundary condition [compare panels (c) and (d)].

To better understand the influence of the boundaries, we consider a complementary analysis, examining $\langle \Delta r^2 \rangle$ at a fixed Δt and varying t_{age}. We choose $\Delta t = 20$ min, where Figs. 3 and 4 show that the particles' average movement decreases with increasing t_{age} in both smooth and rough boundaries. Figure 5 shows the data divided by rough boundary condition [panels (a) and (b)] and smooth boundary condition [panels (c) and (d)], for motion parallel and perpendicular to the boundaries (left and right panels, respectively). The colors indicate different layers, as labeled in panels (e) and (f). The overall decreasing trend of all the curves with larger t_{age} is the signature of aging, with the logarithmic t_{age} axis making apparent that the rate of decrease itself is slower in older samples. The
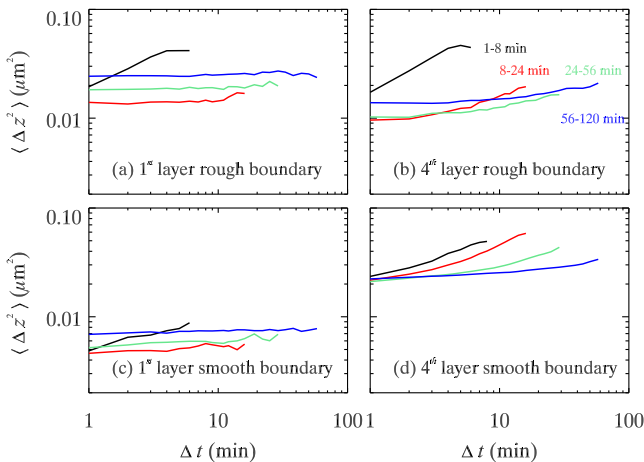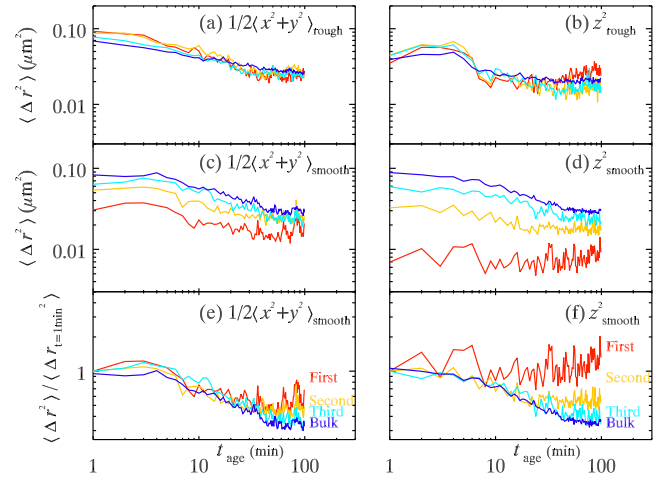

FIG. 5. Average distance particles move over $\Delta t = 20$ min, as a function of aging time t_{age}. The curve colors indicate the layer number as labeled in panels (e) and (f). Panels show data for motions parallel to the boundary ($1/2\langle x^2 + y^2 \rangle$) and perpendicular to the boundary ($\langle z^2 \rangle$) for rough and smooth boundaries as indicated. In panels (e) and (f), the data are normalized by their initial values.

data suggest that the sample is still aging at the longest times observed in our experiment, although even reaching a steady-state for $\Delta t = 20$ min does not preclude the sample from still having an aging signal at longer Δt.

For the rough boundaries [Figs. 5(a) and 5(b)], the data collapse for all layers confirming that the boundary appears to have a negligible influence on the dynamics. However, for the smooth boundary condition, the wall-induced structures bring significant differences for motion parallel to the boundary [Fig. 5(c)] and even larger differences in the perpendicular direction [Fig. 5(d)]. Both types of motion are slower closer to the wall. For the motion perpendicular to the boundary [panel (d)], the motion in the first layer is around ten times smaller than the bulk. Moreover, unlike other layers, we do not observe an aging signal in the first layer—the curve is essentially flat. The lack of observed aging behavior of Δz^2 suggests that this first layer has very slow dynamics. Of course, the perpendicular motion in the first layer is bounded at $z = 0$, but the displacements we observe are much smaller than for the first layer next to the rough wall, which has a similar constraint on perpendicular motion. Our observations of nearly immobile particles with no aging signature in this first layer match results from thin polymer films near attractive silica substrates.[21]

As a different way of understanding how the aging process changes near the smooth boundary, we normalize $\langle \Delta r^2(t) \rangle$ by $\langle \Delta r^2(t_{age} = 1 \text{ min}) \rangle$ as shown in Figs. 5(e) and 5(f). For both motion parallel and perpendicular to the boundary, the data collapse moderately well for $t_{age} \lesssim 10$ min, indicating an initial aging trend. For $t_{age} \gtrsim 10$ min, the first and second layers nearly stop evolving while the other layers are still aging. This is especially true for the z motion [panel (f)].

To further explore the relation between the layering structures and motion perpendicular to the boundary, we define $\langle \Delta z^2_{asym} \rangle$. This is the average of the data of Figs. 5(b) and 5(d) in the asymptotic regime, that is, for $t_{age} \geq 85$ min. The results

FIG. 4. The mean square displacement along the direction perpendicular to the boundary (z) calculated during four different t_{age} regimes as indicated. Data are for (a) 1st layer with a rough boundary, (b) 4th layer with a rough boundary, (c) 1st layer with a smooth boundary, (d) 4th layer with a smooth boundary.
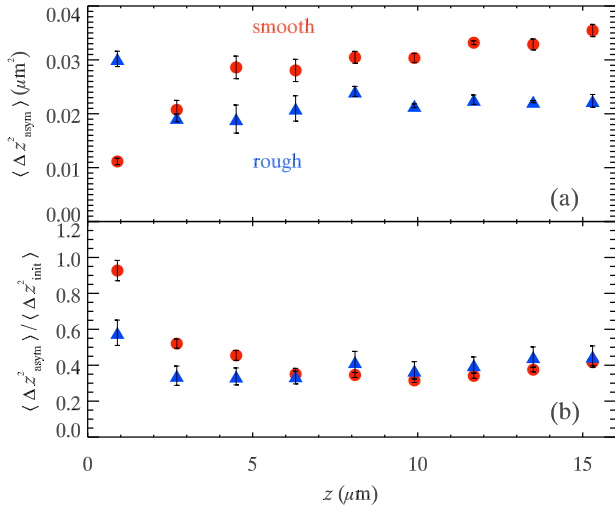
FIG. 6. (a) The t_{age} average of Δz^2 for the last 15 min of Figs. 5(b) and 5(d) plotted as a function of z, with the average done over all particles in a layer (as defined in Fig. 2). The z value is the center of each layer over which the average is taken. (b) The same data normalized by the mean value of Δz^2 for $t_{age} \leq 5$ min. This represents the slowing seen due to aging; the data close to 1.0 show little or no aging behavior. The error bars represent the variability in the results when different ranges for the t_{age}-averaging are used.

are plotted as a function of the distance from the wall in Fig. 6(a). The smooth data (red circles) smoothly increases as z increases. The rough data (blue triangles) are fairly constant, with the exception of the first layer ($z = 0.8$ μm) which is larger. As argued above based on the flatness of the data in Fig. 4(a), this increase in the first layer is likely due to photobleaching than true motion. For $z > 5$ μm, the differences between smooth and rough data are likely due to the image quality which artificially increases the MSD.[79] To account for this, in Fig. 6(b) the data are normalized by the value of $\langle \Delta z^2 \rangle$ averaged over $t_{age} \leq 5$ min. This collapses the data for $z > 5$ μm. These data are related to the amount the dynamics slow as the sample ages, with 1 corresponding to no slowing and smaller values indicating slowing with age. The value close to 1 for the smooth boundary condition indicates that the first layer barely ages, consistent with the similarity of the MSD data of Fig. 4(c) and the horizontal red line in Fig. 5(d). The decrease in the data of Fig. 6(b) as z increases shows a return to the normal aging seen in the bulk.

The qualitative similarity of the rough and smooth data in Fig. 6(b) motivates an attempt to collapse the data by a horizontal shift. Noting that the number density data of Fig. 2(b) look like a horizontally shifted portion of the data of Fig. 2(a), we use the local layer structure as a possible way to explain the dynamical data. We quantify the structure using the standard deviation of $n(z)$ within a layer divided by its mean. Figure 7 shows this nearly collapses the data (to within fluctuations of $\sim$20%) accounting for most of the effect. The data for $\sigma_n/\langle n \rangle \lesssim 0.2$ are essentially the bulk region. Thus the difference in dynamics between the smooth and rough boundaries we observe can be explained by the difference in particle layering that occurs next to these two interfaces.
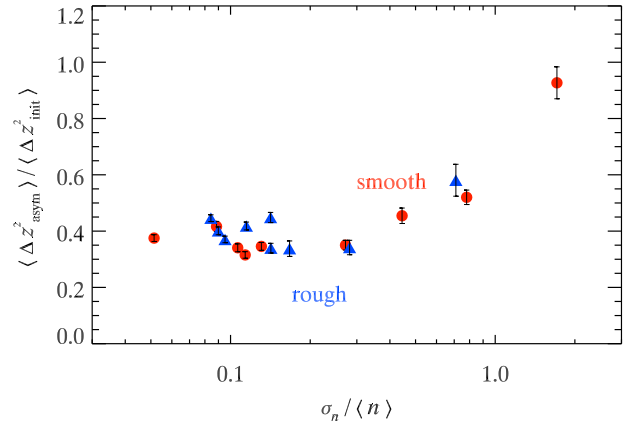

FIG. 7. The large t_{age} motion in z plotted as a function of the standard deviation of number density σ_n over the mean number density $\langle n \rangle$ where these quantities are defined within each layer (see Fig. 2). The data for the vertical coordinate correspond to that of Fig. 6(b).

IV. CONCLUSIONS

In our experiment, we study aging by observing particle motion in a colloidal glass near smooth and rough boundaries. Both samples exhibit aging in their bulk. Near a smooth boundary, the particles form layers against the boundary such that in the two layers closest to the wall, motion is greatly diminished. For a smooth wall, we observe that the influence of the boundary extends up to $\approx$6 layers ($\approx$4 large particle diameters) into the sample. The observations of a gradient in dynamics near the smooth wall are qualitatively similar to prior observations of gradients near interfaces in glassy materials. Direct evidence for gradients in dynamics has been seen in molecular dynamics simulations[10,11,30] and colloidal experiments.[15,28] In other experiments, the influences of the boundaries are inferred from local probes near the boundary (e.g., Ref. 21) or fitting the data to models assuming boundary effects (e.g., Ref. 12).

Here we not only see the gradient in dynamics but also observe that this gradient in dynamics is directly related to a gradient in the structural properties. For a rough boundary, the wall-induced structure is greatly reduced and the dynamics appear more bulk-like near the boundary, being similar to that far into the bulk. By comparing the local dynamics near the rough and smooth boundaries, our results suggest that the dominant factor modifying aging dynamics near a boundary is the structure caused by the presence of the boundary. By presenting a rough amorphous boundary, the structure is more bulk-like and thus the dynamics are more bulk-like. A fruitful area for future work would be to explore boundary textures that have intermediate influences on the layering structure.

These experimental results on colloidal glasses suggest a viable means by which neutral rough amorphous boundaries may be implemented in computer simulations. This is an issue that computational studies on the influence of interfacial effects on local dynamics have been struggling with for more than two decades[5,10,11,30–32,39] and has relevance for the implementation of theoretical point-to-set studies.[40–43] The method employed in the present study creates a rough amorphous boundary by randomly sticking particles to a smooth

wall at approximately 30%-50% surface coverage. The local aging dynamics we observe near such a rough boundary appear nearly bulk-like.

ACKNOWLEDGMENTS

[1] M. Alcoutlabi and G. B. McKenna, "Effects of confinement on material behaviour at the nanometre size scale," J. Phys.: Condens. Matter **17**, R461–R524 (2005).

[2] J. Forrest and K. Dalnoki-Veress, "The glass transition in thin polymer films," Adv. Colloid Interface Sci. **94**, 167–195 (2001).

[3] R. Richert, "Dynamics of nanoconfined supercooled liquids," Annu. Rev. Phys. Chem. **62**, 65–84 (2011).

[4] C. B. Roth and J. R. Dutcher, "Glass transition and chain mobility in thin polymer films," J. Electroanal. Chem. **584**, 13–22 (2005).

[5] J. Baschnagel and F. Varnik, "Computer simulations of supercooled polymer melts in the bulk and in confined geometry," J. Phys.: Condens. Matter **17**, R851–R953 (2005).

[6] M. D. Ediger and J. A. Forrest, "Dynamics near free surfaces and the glass transition in thin polymer films: A view to the future," Macromolecules **47**, 471–478 (2014).

[7] S. Napolitano, E. Glynos, and N. B. Tito, "Glass transition of polymers in bulk, confined geometries, and near interfaces," Rep. Prog. Phys. **80**, 036602 (2017).

[8] G. L. Hunter and E. R. Weeks, "The physics of the colloidal glass transition," Rep. Prog. Phys. **75**, 066501 (2012).

[9] K. Binder, J. Baschnagel, and W. Paul, "Glass transition of polymer melts: Test of theoretical concepts by computer simulation," Prog. Polym. Sci. **28**, 115–172 (2003).

[10] W. Kob, P. Scheidler, and K. Binder, "The relaxation dynamics of a simple glass former confined in a pore," Europhys. Lett. **52**, 277–283 (2000).

[11] P. Scheidler, W. Kob, and K. Binder, "Cooperative motion and growing length scales in supercooled confined liquids," Europhys. Lett. **59**, 701–707 (2002).

[12] J. E. Pye, K. A. Rohald, E. A. Baker, and C. B. Roth, "Physical aging in ultrathin polystyrene films: Evidence of a gradient in dynamics at the free surface and its connection to the glass transition temperature reductions," Macromolecules **43**, 8296–8303 (2010).

[13] P. Z. Hanakata, J. F. Douglas, and F. W. Starr, "Interfacial mobility scale determines the scale of collective motion and relaxation rate in polymer films," Nat. Commun. **5**, 4163 (2014).

[14] R. J. Lang and D. S. Simmons, "Interfacial dynamic length scales in the glass transition of a model freestanding polymer film and their connection to cooperative motion," Macromolecules **46**, 9818–9825 (2013).

[15] P. S. Sarangapani, A. B. Schofield, and Y. Zhu, "Direct experimental evidence of growing dynamic length scales in confined colloidal liquids," Phys. Rev. E **83**, 030502 (2011).

[16] P. S. Sarangapani, A. B. Schofield, and Y. Zhu, "Relationship between cooperative motion and the confinement length scale in confined colloidal liquids," Soft Matter **8**, 814–818 (2012).

[17] F. He, L. M. Wang, and R. Richert, "Confined viscous liquids: Interfacial versus finite size effects," Eur. Phys. J.: Spec. Top. **141**, 3–9 (2007).

[18] D. S. Fryer, R. D. Peters, E. J. Kim, J. E. Tomaszewski, J. J. de Pablo, P. F. Nealey, C. C. White, and W.-l. Wu, "Dependence of the glass transition temperature of polymer films on interfacial energy and thickness," Macromolecules **34**, 5627–5634 (2001).

[19] O. K. C. Tsui, T. P. Russell, and C. J. Hawker, "Effect of interfacial interactions on the glass transition of polymer thin films," Macromolecules **34**, 5535–5539 (2001).

[20] K. Paeng, R. Richert, and M. D. Ediger, "Molecular mobility in supported thin films of polystyrene, poly(methyl methacrylate), and poly(2-vinyl pyridine) probed by dye reorientation," Soft Matter **8**, 819–826 (2012).

[21] R. D. Priestley, C. J. Ellison, L. J. Broadbelt, and J. M. Torkelson, "Structural relaxation of polymer glasses at surfaces, interfaces, and in between," Science **309**, 456–459 (2005).

[22] C. B. Roth, K. L. McNerny, W. F. Jager, and J. M. Torkelson, "Eliminating the enhanced mobility at the free surface of polystyrene: Fluorescence studies of the glass transition temperature in thin bilayer films of immiscible polymers," Macromolecules **40**, 2568–2574 (2007).

[23] C. M. Evans, S. Narayanan, Z. Jiang, and J. M. Torkelson, "Modulus, confinement, and temperature effects on surface capillary wave dynamics in bilayer polymer films near the glass transition," Phys. Rev. Lett. **109**, 038302 (2012).

[24] R. R. Baglay and C. B. Roth, "Communication: Experimentally determined profile of local glass transition temperature across a glassy-rubbery polymer interface with a T_g difference of 80 K," J. Chem. Phys. **143**, 111101 (2015).

[25] J. Wang and G. B. McKenna, "Viscoelastic and glass transition properties of ultrathin polystyrene films by dewetting from liquid glycerol," Macromolecules **46**, 2485–2495 (2013).

[26] D. Christie, C. Zhang, J. Fu, B. Koel, and R. D. Priestley, "Glass transition temperature of colloidal polystyrene dispersed in various liquids," J. Polym. Sci., Part B: Polym. Phys. **54**, 1776–1783 (2016).

[27] K. V. Edmond, C. R. Nugent, and E. R. Weeks, "Influence of confinement on dynamical heterogeneities in dense colloidal samples," Phys. Rev. E **85**, 041401 (2012).

[28] G. L. Hunter, K. V. Edmond, and E. R. Weeks, "Boundary mobility controls glassiness in confined colloidal liquids," Phys. Rev. Lett. **112**, 218302 (2014).

[29] R. R. Baglay and C. B. Roth, "Local glass transition temperature $T_g(z)$ of polystyrene next to different polymers: Hard vs. soft confinement," J. Chem. Phys. **146**, 203307 (2017).

[30] P. Scheidler, W. Kob, and K. Binder, "The relaxation dynamics of a supercooled liquid confined by rough walls," J. Phys. Chem. B **108**, 6673–6686 (2004).

[31] P. Z. Hanakata, B. A. Pazmiño Betancourt, J. F. Douglas, and F. W. Starr, "A unifying framework to quantify the effects of substrate interactions, stiffness, and roughness on the dynamics of thin supported polymer films," J. Chem. Phys. **142**, 234907 (2015).

[32] T. Davris and A. V. Lyulin, "A coarse-grained molecular dynamics study of segmental structure and mobility in capped crosslinked copolymer films," J. Chem. Phys. **143**, 074906 (2015).

[33] F. Varnik and K. Binder, "Shear viscosity of a supercooled polymer melt via nonequilibrium molecular dynamics simulations," J. Chem. Phys. **117**, 6336–6349 (2002).

[34] F. Varnik, J. Baschnagel, and K. Binder, "Static and dynamic properties of supercooled thin polymer films," Eur. Phys. J. E: Soft Matter **8**, 175–192 (2002).

[35] F. Varnik, J. Baschnagel, and K. Binder, "Reduction of the glass transition temperature in polymer films: A molecular-dynamics study," Phys. Rev. E **65**, 021507 (2002).

[36] S. Peter, H. Meyer, and J. Baschnagel, "Thickness-dependent reduction of the glass-transition temperature in thin polymer films with a free surface," J. Polym. Sci., Part B: Polym. Phys. **44**, 2951–2967 (2006).

[37] P. Z. Hanakata, J. F. Douglas, and F. W. Starr, "Local variation of fragility and glass transition temperature of ultra-thin supported polymer films," J. Chem. Phys. **137**, 244901 (2012).

[38] G. D. Smith, D. Bedrov, and O. Borodin, "Structural relaxation and dynamic heterogeneity in a polymer melt at attractive surfaces," Phys. Rev. Lett. **90**, 226103 (2003).

[39] T. Fehr and H. Löwen, "Glass transition in confined geometry," Phys. Rev. E **52**, 4016–4025 (1995).

[40] G. Biroli, J. P. Bouchaud, A. Cavagna, T. S. Grigera, and P. Verrocchio, "Thermodynamic signature of growing amorphous order in glass-forming liquids," Nat. Phys. **4**, 771–775 (2008).

[41] Y.-W. Li, W.-S. Xu, and Z.-Y. Sun, "Growing point-to-set length scales in Lennard-Jones glass-forming liquids," J. Chem. Phys. **140**, 124502 (2014).

[42] G. M. Hocky, L. Berthier, W. Kob, and D. R. Reichman, "Crossovers in the dynamics of supercooled liquids probed by an amorphous wall," Phys. Rev. E **89**, 052311 (2014).

[43] K. Hima Nagamanasa, S. Gokhale, A. K. Sood, and R. Ganapathy, "Direct measurements of growing amorphous order and non-monotonic dynamic correlations in a colloidal glass-former," Nat. Phys. **11**, 403–408 (2015).

[44] D. Hudzinskyy, A. V. Lyulin, A. R. C. Baljon, N. K. Balabaev, and M. A. J. Michels, "Effects of strong confinement on the glass-transition temperature in simulated atactic polystyrene films," Macromolecules **44**, 2299–2310 (2011).

[45] P. Gin, N. Jiang, C. Liang, T. Taniguchi, B. Akgun, S. K. Satija, M. K. Endoh, and T. Koga, "Revealed architectures of adsorbed polymer chains at solid-polymer melt interfaces," Phys. Rev. Lett. **109**, 265501 (2012).

[46] M. Sen, N. Jiang, J. Cheung, M. K. Endoh, T. Koga, D. Kawaguchi, and K. Tanaka, "Flattening process of polymer chains irreversibly adsorbed on a solid," ACS Macro Lett. **5**, 504–508 (2016).

[47] S. Napolitano, S. Capponi, and B. Vanroy, "Glassy dynamics of soft matter under 1D confinement: How irreversible adsorption affects molecular packing, mobility gradients and orientational polarization in thin films," Eur. Phys. J. E: Soft Matter **36**, 1–37 (2013).

[48] K. S. Gautam, A. D. Schwab, A. Dhinojwala, D. Zhang, S. M. Dougal, and M. S. Yeganeh, "Molecular structure of polystyrene at air/polymer and solid/polymer interfaces," Phys. Rev. Lett. **85**, 3854–3857 (2000).

[49] X. Huang and C. B. Roth, "Changes in the temperature-dependent specific volume of supported polystyrene films with film thickness," J. Chem. Phys. **144**, 234903 (2016).

[50] Z. T. Németh and H. Löwen, "Freezing and glass transition of hard spheres in cavities," Phys. Rev. E **59**, 6824–6829 (1999).

[51] L. C. E. Struik, "Physical aging in plastics and other glassy materials," Polym. Eng. Sci. **17**, 165–173 (1977).

[52] W. van Megen, T. C. Mortensen, S. R. Williams, and J. Müller, "Measurement of the self-intermediate scattering function of suspensions of hard spherical particles near the glass transition," Phys. Rev. E **58**, 6073–6085 (1998).

[53] R. D. Priestley, "Physical aging of confined glasses," Soft Matter **5**, 919–926 (2009).

[54] P. Ramírez-González and M. Medina-Noyola, "Aging of a homogeneously quenched colloidal glass-forming liquid," Phys. Rev. E **82**, 061504 (2010).

[55] M. R. Tant and G. L. Wilkes, "An overview of the nonequilibrium behavior of polymer glasses," Polym. Eng. Sci. **21**, 874–895 (1981).

[56] Y. Huang and D. R. Paul, "Physical aging of thin glassy polymer films monitored by gas permeability," Polymer **45**, 8377–8393 (2004).

[57] J. B. Knight, C. G. Fandrich, C. N. Lau, H. M. Jaeger, and S. R. Nagel, "Density relaxation in a vibrated granular material," Phys. Rev. E **51**, 3957–3963 (1995).

[58] P. Richard, M. Nicodemi, R. Delannay, P. Ribiere, and D. Bideau, "Slow relaxation and compaction of granular systems," Nat. Mater. **4**, 121–128 (2005).

[59] D. El Masri, M. Pierno, L. Berthier, and L. Cipelletti, "Ageing and ultra-slow equilibration in concentrated colloidal hard spheres," J. Phys.: Condens. Matter **17**, S3543–S3549 (2005).

[60] V. A. Martinez, G. Bryant, and W. van Megen, "Slow dynamics and aging of a colloidal hard sphere glass," Phys. Rev. Lett. **101**, 135702 (2008).

[61] L. Cipelletti and L. Ramos, "Slow dynamics in glasses, gels and foams," Curr. Opin. Colloid Interface Sci. **7**, 228–234 (2002).

[62] R. E. Courtland and E. R. Weeks, "Direct visualization of ageing in colloidal glasses," J. Phys.: Condens. Matter **15**, S359–S365 (2003).

[63] J. M. Lynch, G. C. Cianci, and E. R. Weeks, "Dynamics and structure of an aging binary colloidal glass," Phys. Rev. E **78**, 031410 (2008).

[64] R. Bandyopadhyay, D. Liang, H. Yardimci, D. A. Sessoms, M. A. Borthwick, S. G. J. Mochrie, J. L. Harden, and R. L. Leheny, "Evolution of particle-scale dynamics in an aging clay suspension," Phys. Rev. Lett. **93**, 228302 (2004).

[65] G. B. McKenna, T. Narita, and F. Lequeux, "Soft colloidal matter: A phenomenological comparison of the aging and mechanical responses with those of molecular glasses," J. Rheol. **53**, 489–516 (2009).

[66] X. Di, K. Z. Win, G. B. McKenna, T. Narita, F. Lequeux, S. R. Pullela, and Z. Cheng, "Signatures of structural recovery in colloidal glasses," Phys. Rev. Lett. **106**, 095701 (2011).

[67] P. Yunker, Z. Zhang, K. Aptowicz, and A. Yodh, "Irreversible rearrangements, correlated domains, and local structure in aging glasses," Phys. Rev. Lett. **103**, 115701 (2009).

[68] L. Antl, J. W. Goodwin, R. D. Hill, R. H. Ottewill, S. M. Owens, S. Papworth, and J. A. Waters, "The preparation of poly(methyl methacrylate) latices in non-aqueous media," Colloid Surf. **17**, 67–78 (1986).

[69] P. N. Pusey and W. van Megen, "Phase behaviour of concentrated suspensions of nearly hard colloidal spheres," Nature **320**, 340–342 (1986).

[70] A. D. Dinsmore, E. R. Weeks, V. Prasad, A. C. Levitt, and D. A. Weitz, "Three-dimensional confocal microscopy of colloids," App. Opt. **40**, 4152–4159 (2001).

[71] T. Narumi, S. V. Franklin, K. W. Desmond, M. Tokuyama, and E. R. Weeks, "Spatial and temporal dynamical heterogeneities approaching the binary colloidal glass transition," Soft Matter **7**, 1472–1482 (2011).

[72] J. C. Crocker and D. G. Grier, "Methods of digital video microscopy for colloidal studies," J. Colloid Interface Sci. **179**, 298–310 (1996).

[73] G. B. McKenna, "Mechanical rejuvenation in polymer glasses: Fact or fallacy?," J. Phys.: Condens. Matter **15**, S737–S763 (2003).

[74] K. W. Desmond and E. R. Weeks, "Influence of particle size distribution on random close packing of spheres," Phys. Rev. E **90**, 022204 (2014).

[75] V. A. Martinez, G. Bryant, and W. van Megen, "Aging dynamics of colloidal hard sphere glasses," J. Chem. Phys. **133**, 114906 (2010).

[76] J. W. Landry, G. S. Grest, L. E. Silbert, and S. J. Plimpton, "Confined granular packings: Structure, stress, and forces," Phys. Rev. E **67**, 041303 (2003).

[77] R. Kjellander and S. Sarman, "Pair correlations of non-uniform hard-sphere fluids in narrow slits and the mechanism of oscillatory solvation forces," J. Chem. Soc. Faraday Trans. **87**, 1869–1881 (1991).

[78] J. Mittal, T. M. Truskett, J. R. Errington, and G. Hummer, "Layering and position-dependent diffusive dynamics of confined fluids," Phys. Rev. Lett. **100**, 145901 (2008).

[79] W. C. K. Poon, E. R. Weeks, and C. P. Royall, "On measuring colloidal volume fractions," Soft Matter **8**, 21–30 (2012).